SILICON POINT CONTACT CONCENTRATOR SOLAR CELLS

R. A. Sinton, Y. Kwark, P. Gruenbaum, R. M Swanson

Stanford Electronics Laboratories, McCullough 204
Stanford, CA 94305 (415)-497-4389

ABSTRACT

Recent advances in silicon concentrator solar cells have resulted in cells with 25% efficiencies at 20 watts/cm^2 of incident sunlight at 26° C. These solar cells are thin, high resistivity cells with an unconventional backside point contact design optimized to operate in high level injection. This paper presents these results and a characterization of some of these cells with respect to wafer thickness. This data verifies predictions from a quasi-three dimensional model which had predicted a critical thickness dependence. A cell optimized for performance at 36 watts/cm^2 incident intensity will be less than 100μm thick.

INTRODUCTION

Silicon concentrator solar cells which have both types of contacts on the backside of the wafer have been shown to have several potential advantages over conventional designs with a single backside contact. A list of these includes elimination of shading loss in the front grid, decreased metal series resistance and additional freedoms in the emitter optimization since the diffusions are far from the regions of maximum photogeneration [1,2].

A backside cell has been optimized for operation under high level injection using a quasi-three dimensional model, [2,3,4]. Additional benefits were found from a backside contact design which presumes that carrier lifetimes exceed several hundred μsecs. Initial experiments resulted in a 20% cell at 8.8 watts/cm^2, 88 suns, of incident sunlight [5]. A simplified version of this cell has recently achieved 23% at 11 watts/cm^2 [6].

This report presents cells with antireflection coatings which are 25% efficient at 20 watts/cm^2 (26 °C). A critical dependence on the cell thickness predicted by the model was investigated by fabricating cells with thicknesses of 100-240μm.

EXPERIMENT

The cells were fabricated on < 100 > float zone n-type 100-200 ohm-cm wafers using processing techniques in which special care was taken to maintain high carrier lifetimes and low surface recombination velocities. The processing schedule was presented in ref. [6]. A cross sectional view of the resulting 0.15 cm^2 cell is shown in Fig 1. The main features of 4 of the cells are listed in table 1. All four of the cells have a 2μm thick metalization which has 13 milliOhms of total series resistance. The contact resistance is predicted to be about 2 milliOhms based on the specific contact resistivities, 1-2$\times 10^{-6}$ Ohm-cm^2 for both N and P type contacts, as determined using Kelvin cross-bridge contact resistance structures. The sheet resistivities for the N and P-type diffusions are 5 and 6 ohms/square, respectively, for the process schedule used.

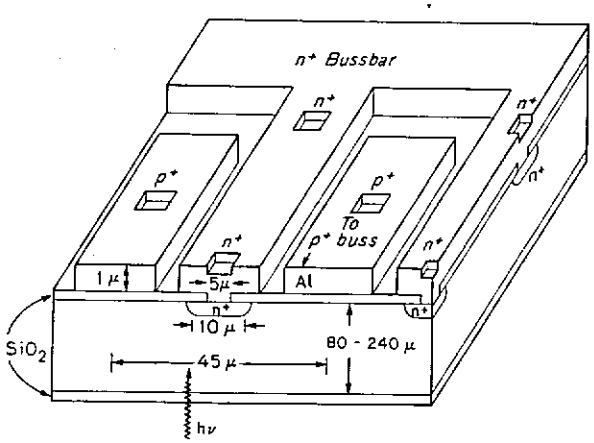

Fig. 1. A cross section of a portion of the solar cell near the busbar for the n$^+$ diffusions. The sunward side oxide (on the bottom here) was thinned on some cells and a double layer antireflection coating was evaporated onto it.

0160-8371/85/0000-0061 $1.00 © 1985 IEEE

In addition to differences in thickness, ranging from 100 to 240μm, there are two types of antireflection coatings on these cells. Cells FT4-2F and FT5-1i have an optically optimized thickness of thermally grown SiO_2 of 1120 Å. Cells FT5-4C and FT6-U have an antireflection coating of 1000 Å MgF_2 over 360 Å TiO_2 on 100-150 Å SiO_2.

Table 1

Cell Characteristics, cell area = .15 cm^2		
Cell I.D.	Thickness	Front Surface Composition
FT4-2F	240μm	1120 A SiO_2
FT5-1i	160μm	1120 A SiO_2
FT5-4C	160μm	$MgF_2/TiO_2/SiO_2$
FT6-U	100μm	$MgF_2/TiO_2/SiO_2$

Results: The illuminated cell characteristics were obtained using a four point electrical measurement in sunlight concentrated by a front surface parabolic mirror. The values given for J_{sc}, the short circuit current, were not taken at 0 volts but at the lowest attainable voltage across our passive load [7]. In the worst case, J_{sc} was taken at a voltage of 595 mV when the maximum power point was at 695 mV for a cell under 47 watts/cm^2 illumination. At lower currents, the cells can be brought much closer to 0 volts.

The curves of efficiency vs. incident power are shown in Fig. 2. with more detailed data given in table 2. Two major features are seen. A comparison of the efficiency of the 160μm cells FT5-1i and FT5-4C indicates that our antireflection coating adds about 1.5 to 2% to the efficiency, boosting the efficiency from about 23% to 25% in the region around 15 watts/cm^2. The second feature is seen by comparing FT4-2F (240μm) with FT5-1i which differ in thickness but not in antireflection coating and similarly comparing FT6-U (100μm) with FT5-1i (160μm). At concentrations over 15 watts/cm^2, efficiencies degrade with increasing cell thickness. At 50 watts/cm^2, this effect costs 1-2% in cell efficiency in going from 100 to 160μm thickness. The efficiency at 440 suns decreases from 20% to 17% when the wafer thickness is increased from 160μm to 240μm. Notice that since all these cells have the same metalization, the I^2R power loss in the metal does not enter strongly into a comparison between cells at a given incident intensity. However, the I^2R loss in the metalization in all four cells represents a 1% loss in efficiency near 500 suns and could be virtually eliminated using thicker metal or a two level metal design as in ref. [5].

A plot of normalized normalized responsivity vs. incident intensity for the four cells is given in Fig 3.; responsivity is defined as amps at short circuit per incident watt of sunlight. The values are normalized to be 1 at

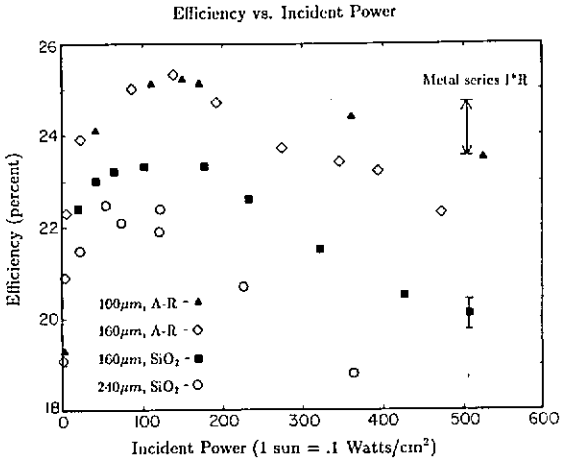

Fig. 2. Efficiency vs incident intensity for four cells. Each cell is designated with an antireflection coating (A-R) or 1120 Å SiO_2. A representative error bar is shown.

low intensity. This is a measure of the collection quantum efficiency as a function of incident intensity. A loss in quantum efficiency is seen at high incident intensities. This loss is most severe in the 240μm cell which has less than 80% of the responsivity at 437 suns as it has at low incident concentrations of sunlight. A comparison of fig. 2 and fig. 3. indicates that most of the loss in efficiency in the thick cell is accounted for by the loss in quantum efficiency at high incident concentrations.

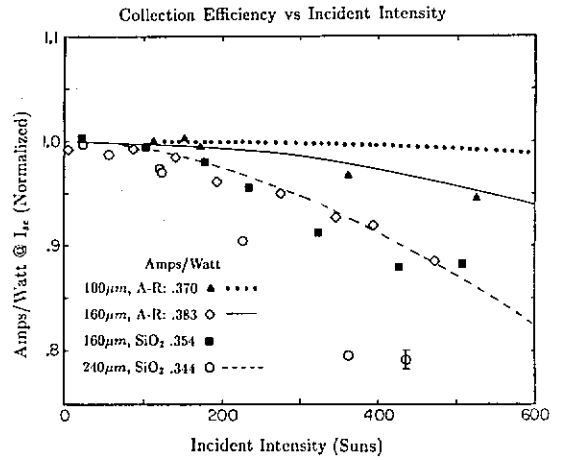

Fig. 3. Normalized responsivity, (amps/incident watt), vs. incident intensity. The normalization for each curve is indicated in the key.

Table 2

Incident Power	Efficiency	J_{sc}	V_{oc}	T	V_{mp}	J_{mp}	FF
Watts/cm²	%	Amps/cm²	mV	°C	mV	A/cm²	
160 micron cell FT5-1i							
2.1	22.4	0.746	764	27	669	0.709	0.83
6.54	23.2	2.30	790	27	691	2.20	0.83
17.8	23.3	6.18	808	28	712	5.82	0.83
32.3	21.5	10.4	816	28	699	9.94	0.81
50.8	20.1	15.9	823	29	682	15.0	0.78
160 micron cell FT5-4C							
0.111	19.1	0.043	665	26.7	522	0.0405	0.76
0.640	22.3	0.246	730	26.8	608	0.235	0.81
2.43	23.9	0.936	768	26.5	678	8.56	0.82
8.79	25.0	3.34	798	26.0	700	3.13	0.84
14.0	25.3	5.28	808	25.3	713	4.94	0.84
19.4	24.7	7.14	812	26.2	714	6.70	0.83
47.2	22.3	16.0	825	27.1	692	15.2	0.79
100 micron cell FT6-U							
0.102	19.3	0.038	674	25.2	541	0.0364	0.77
4.29	24.1	1.56	788	24.9	686	1.51	0.84
11.2	25.1	4.13	808	25.6	710	3.96	0.85
15.1	25.2	5.59	813	26.2	716	5.33	0.84
17.2	25.1	6.31	815	26.2	708	6.09	0.83
36.3	24.4	13.0	828	26.7	713	12.4	0.82
52.6	23.5	18.4	833	26.5	710	17.4	0.81
240 micron cell FT4-2F							
2.30	21.5	.776	763	24	662	.732	0.82
5.59	22.5	1.88	785	22	685	1.81	0.84
12.2	21.9	4.04	799	23	3.91	685	0.83
36.3	18.8	10.1	817	21	9.74	699	0.83
43.7	17.3	11.9	817	22	11.2	676	0.78
	±0.3	±1%	±2 mV	±0.5 C	±2 mV	±1%	±0.01

The plots of V_{oc} vs. incident intensity are shown in Fig. 4. Thinner cells have higher open circuit voltages, especially at high concentrations. The temperatures for the individual points are given in table 2.

An important result for cell modeling is a determination of an effective carrier lifetime by means of an open-circuit voltage decay technique. A flashlamp was used to illuminate the cell and the slope of the voltage decay determined. The lifetime was then calculated from the relation:

$$\frac{1}{\tau_{eff}} = \frac{q}{2kT}\frac{dV}{dt}$$

where τ_{eff} was measured at an open circuit voltage of 600 mV for cells of each of the four thicknesses. At this carrier density, about $10^{15}/cm^2$, the recombination will be dominated by the surface and bulk Shockley-Read-Hall recombination which is assumed to be linear in carrier density. The lifetimes determined in this manner were 950 μsec for the 240μm cell, 600-700 μsec for 160 μm cells, and 350 μsec for the 100μm cells.

MODELING

The modeling curves in Fig. 3 and Fig. 4 are from a quasi-three dimensional model which describes the carrier densities in the quasi neutral base as a function of emitter saturation current, J_o, surface recombination velocity, bulk carrier lifetimes, and cell geometry. An ambipolar Auger coefficient of 4.0×10^{-31} cm^6/sec was used [8], and the diffusion coefficient was assumed to

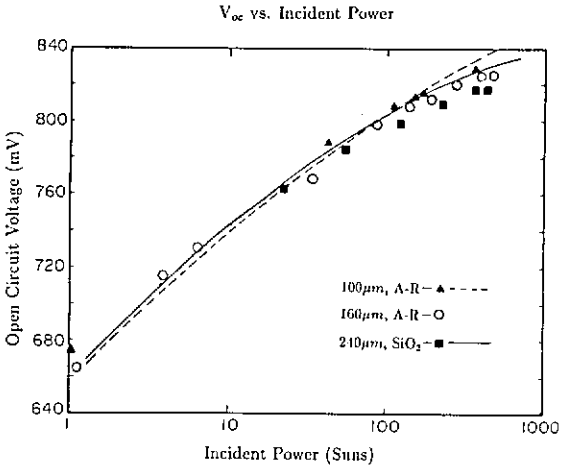

Fig. 4. Open circuit voltage vs. incident intensity. Each curve is taken at approximately constant temperature ±1 °C. The exact temperatures are listed in table 2.

be the same as in doped material from ref. [9]. The parameters used are listed in table 3.

The surface recombination velocity resulting from our processing schedules is typically measured to be less than 15 cm/sec [10]. The model is sensitive to this parameter so it is useful to determine an upper bound for the actual surface recombination velocity on the devices. This can be done by attributing all of the recombination in the cell to surface recombination. This is a good approximation for carrier densities less than $10^{15}/cm^3$, or V_{oc} less than 600 mV, since the J_o and Auger recombination components are small at this carrier density. Then the effective lifetime measured by the V_{oc} implies an upper limit on the surface recombination velocity S given by

$$S = \frac{\text{Wafer Width}}{2\tau_{eff}}$$

For the lifetimes and wafer thicknesses in this experiment, this gives values of the surface recombination velocity of 13.0 ± 1.5 cm/sec. This is a strong indication that the cells have a surface recombination velocity of about 13 cm/sec and negligible bulk recombination. The cell characteristics are relatively independent of the bulk lifetime since it is so high in these devices. For the

Table 3

Modelling Parameters		
Parameter	Symbol	Assumed value
Bulk Shockley-Read Hall lifetime	τ	2 msec
Surface Recombination Velocity	S	15 cm/sec
Ambipolar Auger Coefficient	C_A	4.0×10^{-31} cm^6/sec
Emitter Saturation Current	J_o	4.5×10^{-13} Amps/cm^2

modeling shown here, the surface recombination velocity was assumed to be 15 cm/sec and the bulk carrier lifetime assumed to be 2 msec. The J_o values have been determined to be 4.5×10^{-14} amps/cm^2 for both the N and P-type diffusions for these processing schedules using one dimensional structures in [11]. The model is more fully described in refs [2,3,4].

DISCUSSION

From the curves of efficiency, responsivity, and V_{oc} vs. incident intensity, fig 2-4, it appears that the major features in the efficiency vs. incident intensity curve are determined by the roll-off in quantum efficiency of collection at higher intensities and in thicker cells. In the model, this quantum efficiency decreases as the carrier density increases at high incident concentrations of sunlight. This is due to the nonlinear recombination mechanisms which occur in these cells which operate in high level injection. The thickness dependence enters because of the higher carrier densities which occur in the front of thick cells compared to thin cells for the same incident intensity [2,4]. For example, the modelling for the data presented here indicates that at the maximum power point for 320 suns the loss in quantum efficiency is 57% auger recombination, 9% emitter recombination, and 24% surface recombination in the 240μm cell. In the 100 μm cell at 320 suns, 15% is auger, 41% is emitter, and 37% surface. Only the Auger components would show up as a deviation from unity in Fig. 3. This is because the surface and bulk terms are assumed to be linear in carrier density and the emitter recombination is negligible when the carrier density is very near zero as occurs under short circuit current conditions.

Although the trend in the data is predicted by the modeling results, some quantitative discrepancies appear for the results using the current set of parameters. Particularly, the magnitude of the loss in quantum efficiency is underestimated by the model by about a factor of two or more at the highest intensities measured, 500 suns. A variety of effects could be proposed to explain this discrepancy, such as non-linear recombination terms other than bulk Auger recombination or a necessity to revise the mobilities downward from the majority carrier values measured in doped material, [9]. This would result in higher carrier densities in the front of the cells under short circuit current conditions which would increase the losses due to Auger recombination.

Another more subtle point is illustrated in Fig 3. by the values for the responsivity at low concentration for the four cells, shown in amps/watt in the key. These values depend primarily on the type of antireflection coating. The cells with antireflection coatings have higher responsivities. However, a comparison of the 100 μm and 160μm cells, both with the antireflection coating, shows that the thinner cell has a lower responsivity. This is probably due to a loss in photogeneration by near bandgap light in the thin cell especially since the Al backside reflector only has 60% coverage. This effect will provide a limit to the extent to which gains can be made in reducing the loss in quantum efficiency at high incident intensities by reducing the wafer thickness.

The higher open circuit voltages, seen in Fig 4., occur in thinner cells because even under open circuit conditions there is a particle flux down a density gradient from the illuminated frontside to the backside of the cell. In the 100μm cell the recombination at 320 suns is 69% due to emitter recombination and 23% due to Auger recombination while the thick cell has 43% emitter and 46% Auger. So in all of these cells a gradient in carrier density exist all the way to the back of the cell where the emitter recombination occurs. The drop in carrier density from the front to the back of the cell is proportional to the cell thickness and this gradient. The open circuit voltage is reduced as this drop increases.

Future improvements in efficiency for these cells are expected by addressing four of the problems discussed above. About 1% of improvement in absolute cell efficiency at 500 suns can be gained by eliminating the metal series resistance. Texturizing the cells will increase the photogeneration by near bandgap light and allow even thinner cells which will reduce the Auger recombination. In addition to these improvements, research into advanced emitter design promises a reduction in the emitter recombination, [12]. These improvements promise to push the efficiencies of these cells towards 30%.

CONCLUSIONS

The first silicon solar cells to show efficiencies of 25% have been demonstrated. A strong thickness dependence was observed which causes a loss in quantum efficiency at high incident intensities of sunlight. This effect indicates that the cells should be made as thin as permitted by optical generation constraints.

Acknowledgements

The authors would like to thank W. D. Eades, S. Beckwith, and R. A. Crane for the development of the high lifetime facility and processing techniques; as well as the faculty and staff of the Stanford Integrated Circuits Lab. This work was supported by EPRI Contract RP-790-2.

REFERENCES

1. R. J. Schwartz, "Review of Silicon Solar Cells for High Concentrations", Solar Cells, Vol 6, pp. 17-38, (1982).

2. R. M. Swanson, "Point-Contact Solar Cells: Modeling and Experiment", Solar Cells, to be published.

3. R. M. Swanson, "Point Contact Silicon Solar Cells", Electric Power Research Institute Rep. AP-2859, May 1983.

4. R. M. Swanson, this proceedings.

5. R. M. Swanson, S. K. Beckwith, R. A. Crane, W. D. Eades, Y. H. Kwark, R. A. Sinton, and S. E. Swirhun, "Point Contact Silicon Solar Cells", IEEE Trans Electron Devices, ED-31, NO. 5, pp 661-664, May 1984.

6. R. A. Sinton, Y. Kwark, S. Swirhun, and R. M. Swanson, "Silicon Point Contact Concentrator Solar Cells", IEEE Elec Dev. Letters, Vol. EDL-6 No. 8, August 1985, pp. 405-407.

7. R. A. Crane, R. A. Sinton, R. R. King and R. M. Swanson, this proceedings.

8. K. G. Svantesson and N.G. Nilsson, "The Temperature Dependence of the Auger Recombination Coefficient in Silicon," J.Phys. C: Solid State Physics, Vol 12, 1979, pp. 5111-5120.

9. N. D. Arora, J. R Hauser, and D. J. Roulston, "Electron and Hole Mobilities in Silicon as a Function of Concentration and Temperature," IEEE Trans Electron Devices ED-29(2), pp 292-295, Feb. 1982.

10. Wendell D. Eades, R. M Swanson, "Calculation of the Surface Generation and Recombination Velocities at the Si-SiO_2 Interface", J. Appl. Phys., 15 Nov 1985.

11. D. E. Kane, and R. M Swanson, "Measurement of Emitter Saturation Current by a Contactless Photoconductivity Decay Method", This Proceedings.

12. Young Kwark, R. A. Sinton, and R. M. Swanson, This Proceedings.